Conformational Features of Human Melanin-Concentrating Hormone: An NMR and Computational Analysis

Rosa Maria Vitale,[b] Laura Zaccaro,[a] Benedetto Di Blasio,[b] Roberto Fattorusso,[b] Carla Isernia,[b] Pietro Amodeo,[c] Carlo Pedone,[a] and Michele Saviano*[a]

The conformational features of human melanin-concentrating hormone (hMCH) [Asp1-Phe2-Asp3-Met4-Leu5-Arg6-cyclo-(S—S)(Cys7-Met8-Leu9-Gly10-Arg11-Val12-Tyr13-Arg14-Pro15-Cys16)-Trp17-Gln18-Val19], in water and in a CD_3CN/H_2O (1:1 v/v) mixture at 298 K, have been determined by NMR spectroscopy followed by simulated annealing and molecular dynamics analyses to identify conformer populations. Backbone clustering analysis of NMR-spectroscopy-derived structures in the 7 – 16 peptide region led to the identification of a single representative structure in each solvent. Both root mean square deviation clustering and secondary structure analysis of the final conformers in both solvents show substantial convergence of most conformers into a single fold in the 4 – 17 region, with a limited variability around Gly10 and Tyr13 on going from CD_3CN/H_2O to pure water. The main feature deduced from the analysis of secondary structures is the occurrence of an N-terminal α helix of variable length, which spans an overall residue range of 2 – 9. A comparative analysis in the two solvents highlights that these structures are substantially different from that reported in the literature for the cyclic MCH(5 – 14) subunit of salmon MCH, which was used to perform a molecular characterization of the MCH/receptor complex. Our conformational data call for a critical revision of the proposed MCH/receptor complex model.

KEYWORDS:

conformation analysis · hormones · molecular dynamics · NMR spectroscopy · simulated annealing

Introduction

Melanin-concentrating hormone (MCH), a hypothalamic, heterodetic, cyclic peptide, was initially identified in teleost fish as a regulator of pigmentary changes in background adaptation.[1, 2] MCH was later also found in mammals, in which it plays a particular role in the regulation of food intake behaviour and associated pathologies such as obesity.[3–6] This peptide also appears to be involved in numerous biological functions, such as regulation of the hypothalamic – pituitary – adrenal axis and energy balance.[6–9] Considerable interest has been focused on the role of MCH in regulation of feeding behaviour, because pharmacological and genetic evidence in rodents suggests that compounds capable of mimicking or inhibiting the action of MCH might be useful in the treatment of eating disorders.[10]

An MCH-specific receptor, found mainly in the hypothalamus, has been detected in humans and recognized as a member of the G-protein-coupled receptors (MCH-1R).[11–16] Recently, a second receptor specific for human MCH has been identified and named hMCH-2R.[17–19] MCH-2R has approximately 38% sequence identity with MCH-1R. The discovery of the MCH-1R receptor was the starting point for the identification of the ligand binding domains on the receptor protein, the design of a molecular model of the MCH receptor, and the docking of the cyclic MCH ligand into the putative transmembrane binding domain.

Several studies have been carried out on human MCH peptide (hMCH; Scheme 1) in order to determine the residues important for receptor binding.[11, 20–23] In particular, these studies underline the importance for biological activity of the residues Arg6, Met8, Arg11, and Tyr13, and also of the disulfide S—S bridge between the Cys residues.[16] Recently, the biological activity of a peptide incorporating the hMCH cyclic segment (6 – 16) was report-

$$D^{1}\,F\,D\,M\,L\,R\,C\,M\,L\,G\,R\,V\,Y\,R\,P\,C\,W\,Q\,V^{19}$$

$$D^{1}\,T\,M\,R\,C\,M\,V\,G\,R\,V\,Y\,R\,P\,C\,W\,Q\,V^{17}$$

Scheme 1. *Amino acid sequences of human (top) and salmon (bottom) MCHs.*

[a] *Dr. M. Saviano, Dr. L. Zaccaro, Prof. C. Pedone*
Istituto di Biostrutture e Bioimmagini CNR
via Mezzocannone 6, 80134 Napoli (Italy)
Fax: (+39) 081-5514305
E-mail: saviano@chemistry.unina.it

[b] *Dr. R. M. Vitale, Prof. B. Di Blasio, Prof. R. Fattorusso, Prof. C. Isernia*
Dipartimento di Scienze Ambientali
Seconda Università di Napoli
via Vivaldi 43, 81100 Caserta (Italy)

[c] *Dr. P. Amodeo*
Istituto di Chimica Biomolecolare, CNR
via Campi Flegrei 34, Comprensorio "A. Olivetti"
80070 Pozzuoli, Napoli (Italy)

Supporting information for this article is available on the WWW under http://www.chembiochem.org or from the author.

ed.[23, 24] This peptide showed biological activity identical to that of full-length hMCH for both receptors (MCH-1R and MCH-2R), which indicates that the N-terminal sequence (1 – 5) is not important for binding to receptors. Despite these numerous studies, only one conformational investigation, on salmon MCH (Scheme 1), by NMR spectroscopy and molecular dynamics (MD) has been reported in the literature.[25, 26] This analysis, carried out in D_2O and dimethyl sulfoxide (DMSO) on the cyclic MCH(5 – 14) subunit, showed only intraresidue and a few adjacent-residue connectivities in D_2O and a small number of interresidue 1D NOE enhancements in DMSO. In addition, the MD analysis was obtained as the product of a 50-ps trajectory, a computing time insufficient to analyze the conformational space in detail. This study indicated that the Tyr11 phenolic hydrogen atom is close to the Cys5 and Met6 carbonyl oxygen atoms. This important structural feature may provide the hydrogen bond that is necessary to stabilize the entire peptide conformation.

Recently, the complex of the MCH receptor (modeled on bacteriorhodopsin) and hMCH (constructed from the MD and NMR studies of salmon MCH[23, 25]) was described.[27] This model showed a direct interaction between the side chains of Asp123 in the receptor and Arg11 in MCH as a key requirement for agonist-mediated receptor activation.

In view of the fact that the molecular modeling was carried out by conformational studies on salmon MCH, it is crucial to obtain detailed information on the conformational behaviour of hMCH in order to validate the proposed model.

In this paper we describe a high-field 2D-NMR analysis of hMCH in water and in a CD_3CN/H_2O (1:1 v/v) mixture at 298 K, followed by simulated annealing (SA) and MD analyses to identify conformer populations. In addition, we report the results of a circular dichroism (CD) investigation under the same solvent conditions as used for NMR experiments.

Results

Peptide synthesis

The linear precursor of hMCH peptide was synthesized by the solid-phase method by use of standard 9-fluorenylmethoxycarbonyl (Fmoc) chemistry. The overall yield of the peptide cleaved from the resin by trifluoroacetic acid (TFA) treatment was 79%. Cyclization of the linear product was achieved by air oxidation at room temperature and the cyclic peptide was purified by reversed-phase high performance liquid chromatography (RP-HPLC). The yield of the final product was 8%. The purity and identity of the resulting hMCH peptide were confirmed by analytical RP-HPLC and MALDI-TOF mass spectrometry.

CD analysis

The conformational properties of the hMCH peptide were preliminarily investigated by CD spectroscopy (Figure 1). In order to study the conformational preferences of the peptide under the same solvent conditions as used in the NMR experiments, the CD spectrum was recorded in CH_3CN/H_2O (1:1 v/v).

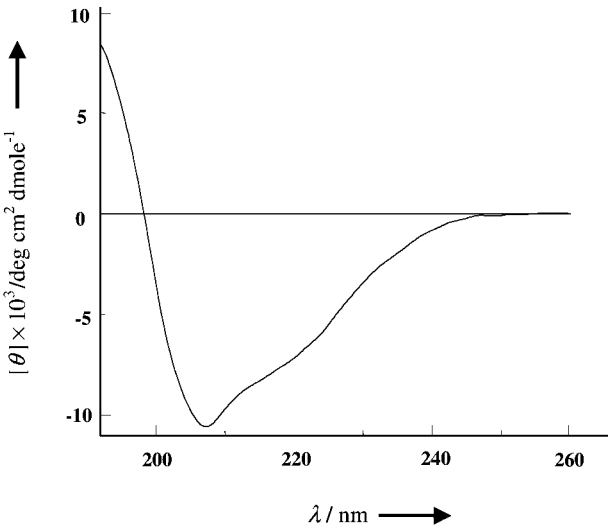

Figure 1. *CD spectrum of the hMCH peptide in CH_3CN/H_2O (50:50 v/v). [θ] is expressed as mean residue molar ellipticity.*

Analysis of the CD spectrum shows some secondary structure content. Spectral deconvolution was performed with the aid of the SELCON3, CONTIN, and CDSSTR programs.[28] The averaged secondary structure percentages were 19%, 22%, 28%, and 31% for helical, turn, extended, and random coil conformations, respectively.

NMR analysis

Spin system identification and assignment of individual resonances of hMCH in H_2O and CD_3CN/H_2O solutions were carried out by using a combination of TOCSY and DQF-COSY spectra.[29, 30] Sequence-specific assignment was obtained by NOESY experiments,[31] according to the standard procedures.[32] Proton chemical shifts for all the resonances at 298 K and in both solvent systems are listed in Table 1.

The 1D spectra show sharp and well-resolved resonances both in H_2O and CD_3CN/H_2O solutions. Interestingly, the amide NH proton resonance of Phe2 resonates at low field in both solvents, while the NH proton signals of the Val12, Trp17, Gln18, and Val19 residues remain at high field. The other NH protons are spread over 8.5 – 9.0 ppm in CD_3CN/H_2O and 8.5 – 9.2 ppm in H_2O. However, some overlap is observed in the amide proton region of the spectrum in water, which produces nearly identical NH proton chemical shifts for residues 17 – 19.

^3J(NH,αCH) coupling constants extracted from the 1D spectrum and from DQF-COSY are reported in Table 2, along with temperature gradients. The temperature variations of amide proton signals in CD_3CN/H_2O and in H_2O were measured over the 298 – 310-K range and the plots were found to be linear; a positive gradient was found for Trp17 in CD_3CN/H_2O. The amide protons of residues 5, 10, 12, and 18 showed lower values in CD_3CN/H_2O, those of residues 12 and 18 in H_2O. This behavior reveals minor overall structural order in the 5 – 10 region in H_2O if compared to the CD_3CN/H_2O medium.

As far as the Arg14 – Pro15 tertiary peptide bond conformation is concerned, similar behaviour is observed in both solvents.

Table 1. ^1H NMR chemical shifts for the hMCH peptide in H_2O/CD_3CN (50:50 v/v) and in H_2O at 298 K.

	H_2O/CD_3CN					H_2O				
AA	NH	αCH	βCH	γCH	Others	NH	αCH	βCH	γCH	Others
Asp1	-	4.55	3.00/2.79			-	4.19	2.83/2.77		
Phe2	8.63	4.53	3.14		2,6H 7.17	8.71	4.60	3.08/3.00		2,6H 7.12
					3,4,5H 7.08					3,4,5H 6.73
Asp3	8.12	4.50	2.72			8.37	4.57	2.79/2.70		
Met4	8.10	4.3	2.05	2.59/2.52	εCH_3 1.68	8.22	4.36	2.06/1.97	2.55/2.48	εCH_3 1.80
Leu5	7.80	4.20	1.66	1.33	δCH_3 0.89/0.94	8.07	4.32	1.68	1.59	δCH_3 0.88/0.86
Arg6	7.87	3.95	1.72	1.62/1.50	NH 7.23 δCH_2 3.07	8.12	4.44	1.65	1.56/1.45	NH 7.05 δCH_2 2.98
Cys7	8.00	4.50	3.18/3.06			8.56	4.68	3.11/2.92		
Met8	8.09	4.40	2.06	2.59/2.49	εCH_3 1.72	8.40	4.55	1.92/1.75	2.22	εCH_3 1.57
Leu9	7.99	4.34	1.70	1.62	δCH_3 0.86	8.44	4.42	1.59/1.42	1.48	δCH_3 0.85
Gly10	7.96	3.90				8.69	3.72/3.94			
Arg11	7.92	4.07	1.88/1.73	1.58	NH 7.17 δCH_2 3.16	8.52	4.22	1.93/1.74	1.59	NH 7.15 δCH_2 3.16
Val12	7.54	4.10	2.01	0.79		7.66	4.21	2.08	0.86	
Tyr13	7.88	4.57	2.98/2.89		2,6H 7.08 3,5H 6.76	8.32	4.73	2.86		2,6H 7.02 3,5H 6.74
Arg14	7.76	4.44	1.72	1.57/1.46	NH 7.12 δCH_2 3.09	8.27	4.56	1.72	1.53/1.46	NH 7.06 δCH_2 3.08
Pro15	-	4.3	2.01/1.46	1.86	δCH_2 3.53/3.36	-	4.35	2.08/1.36	1.89	δCH_2 3.60/3.36
Cys16	8.18	4.43	3.02/2.92			8.46	4.44	3.05/2.90		
Trp17	7.56	4.65	3.24		2H 7.17	7.85	4.62	3.31/3.24		2H 7.24
					4H 7.56					4H 7.56
					5H 7.05					5H 7.11
					6H 7.16					7H 7.46
					7H 7.43					6H 7.21
					NH 10.0					NH 10.2
Gln18	7.72	4.30	1.97/1.75	2.14/2.03	δNH_2 —	7.85	4.25	1.93/1.66	2.01/1.89	δNH_2 —
Val19	7.69	4.14	2.12	0.93		7.86	4.09	2.13	0.88	

Table 2. $^3J(NH,\alpha CH)$ vicinal coupling constants and temperature coefficients for the amide NH protons of the hMCH peptide in H_2O/CD_3CN (50:50 v/v) and H_2O at 298 K.[a]

	H_2O/CD_3CN			H_2O		
AA	$\Delta\delta/\Delta T$	$^3J(NH,\alpha CH)$	ϕ	$\Delta\delta/\Delta T$	$^3J(NH,\alpha CH)$	ϕ
Phe2	–	6.3	−165; −80; 40; 80	−5.8	6.8	−160; −80; 50; 70
Asp3	−3.7	6.0	−165; −75; 40; 80	−6.7	6.9	−160; −80; 60
Met4	−4.7	5.8	−170; −75; 35; 85	−6.8	6.3	−165; −80; 40; 80
Leu5	−2.6	5.9	−170; −75; 35; 85	−6.0	6.3	−165; −80; 40; 80
Arg6	−5.4	6.0	−165; −75; 40; 80	−7.0	6.9	−160; −80; 60
Cys7	−3.5	6.4	−165; −80; 40; 80	−9.5	8.2	−150; −95
Met8	−5.7	6.8	−160; −80; 50 ;70	−7.8	8.0	−150 ; −90
Leu9	−4.6	6.9	−160; −80; 60	−8.3	8.3	−150; −95
Gly10	−2.9	–	–	−12.0	–	–
Arg11	−4.1	7.1	−160; −85	−9.3	7.0	−160; −80; 60
Val12	−3.4	8.4	−145; −95	−3.5	8.6	−145; −95
Tyr13	−6.5	7.9	−150; −90	−8.8	6.1	−165; −75; 40; 80
Arg14	−3.5	6.5	−165; −80; 40; 80	−8.5	8.1	−150; −90
Cys16	−6.5	6.3	−165; −80; 40; 80	−9.1	6.9	−160; −80; 60
Trp17	0.67	7.8	−150; −90	−6.7	7.4	−155; −85
Gln18	−2.5	7.8	−150; −90	−2.5	7.4	−155; −85
Val19	−4.4	8.4	−145; −95	−6.7	7.9	−150; −90

[a] Coupling constants are given in Hz, temperature coefficients in ppb K^{-1}, and ϕ in degrees.

Indeed, a *trans* conformation is adopted in CD_3CN/H_2O solution, as determined from diagnostic $H_{\alpha i}/H_{\delta i+1}$ and $HN_i/H\delta_{i+1}$ cross-peaks between the Arg14 and Pro15 residues in the NOESY spectrum. This peptide bond is also *trans* in H_2O solution, as shown by $H\beta_i/H\delta_{i+1}$ cross-peaks between the Arg14 and Pro15 residues in the NOESY spectrum, since the characteristic $H_{\alpha i}/H_{\delta i+1}$ and $HN_i/H\delta_{i+1}$ cross-peaks are not detectable.

The amide proton regions of the 2D NOESY spectra in H_2O and CD_3CN/H_2O solutions are shown in Figure 2. They both show some strong HN_i/HN_{i+1} NOE cross-peaks, indicative of a helical content in solution. In CD_3CN/H_2O solution, four HN_i/HN_{i+1} connectivity ranges have been assigned to Phe2 – Asp3, Met4 – Met8, Arg11 – Tyr13, and Cys16 – Gln18; pattern breaks at Asp3 – Met4 and Leu9 – Arg11 are due to cross-peak overlaps. In H_2O the NOESY amide proton region shows the following HN_i/HN_{i+1} connectivity ranges: Phe2 – Asp3, Met4 – Leu5, Arg6 – Cys7, Leu9 – Tyr13 and Cys16 – Trp17. To estimate similarities and differences between the peptide conformations in the two solvents, a comparative analysis of NOE effects was performed. This analysis highlighted that, although the average intensity of

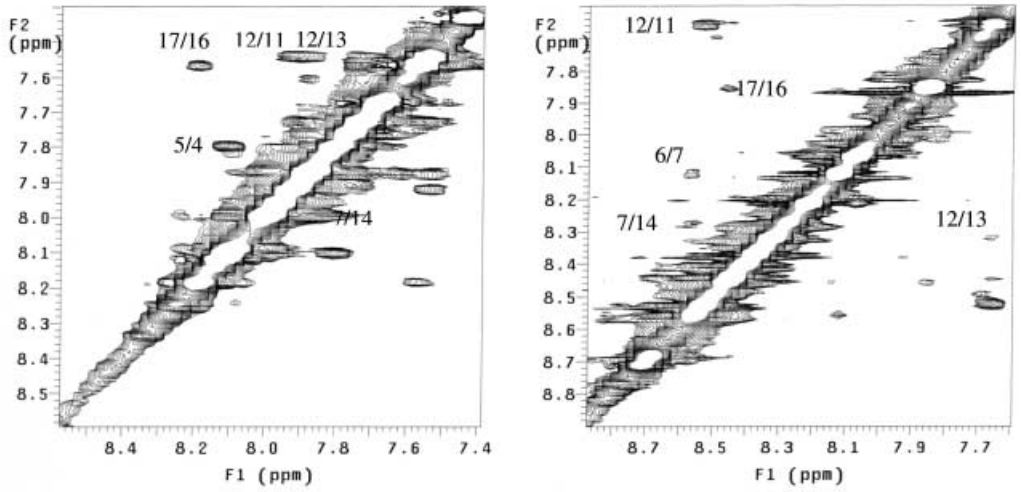

Figure 2. *NOESY spectra (200 ms) recorded at 600 MHz in CD_3CN/H_2O (1:1 v/v) (left) and in H_2O (right) for the hMCH peptide; the amide NH proton region is shown.*

NOEs in water appears to be reduced, the signal pattern is strikingly similar to that in CD_3CN/H_2O. Interestingly, the long-range NOE correlations HN – HN 9 – 12, 7 – 14, 10 – 16, and Hβ/Hδ 6 – 13 are retained in the two different environments, which suggests an intrinsic conformational preference for the peptide.

Computational analysis

A total of 122 (in CD_3CN/H_2O) or 98 (in H_2O) observed NOEs, mostly sequential or intraresidue, were used in structure calculations. Distance restraints derived from intraresidue, sequential, and medium-range NOEs (see the Supporting Information) were introduced in SA torsion-space calculations performed by use of the DYANA package.[33] The best 20 structures in terms of root mean square deviation (RMSD) were selected from the 100 structures sampled in torsion space simulated annealing/energy minimization (TSSA/EM) calculations for each solvent. These conformers have no dihedral restraint violations and no distance restraint violations greater than 0.2 Å.

Backbone clustering analysis in the 7 – 16 sequence region led to the identification of a single representative structure in each solvent. This was subjected to the Cartesian space simulated annealing (CSSA)/EM protocol, which produced 50 new conformers from each starting structure.

The most relevant result from preliminary structural analyses is the substantial similarity of the backbone conformations in CD_3CN/H_2O and in H_2O observed by both computational procedures. Both RMSD clustering and secondary structure analysis of TSSA/EM and CSSA/EM conformers in both solvents show substantial convergence of most conformers into a single fold in the 4 – 17 region (Figure 3 and Figure 4), with a limited variability around Gly10 and Tyr13 on going from CD_3CN/H_2O to pure water (see the Supporting Information).

Analysis of secondary structures shows the occurrence of an N-terminal α helix of variable length that spans residues 2 – 9. Analysis of the residue distribution in the helical conformation was performed by classifying conformers on the basis of the observed helical range and by grouping in the same class all ranges differing by one residue in the starting and/or in the final position (i.e., range *i*/*j* – *k*/*l* potentially includes ranges *i* – *k*, *i* – *l*, *j* – *k*, and *j* – *l*). In particular, in CD_3CN/H_2O, CSSA/EM gives the following populations of helical conformers (given in parentheses as percentages of the total conformers for each observed range): 2/3 – 7 (42%), 2 – 8 (24%), 2 – 9 (18%), 5 – 8 (12%), 4 – 9 (2%), 2 – 5 (2%); in TSSA/EM the distribution is: 5/6 – 8/9 (40%), 4 – 7 (5%), 3 – 7 (5%). In water, the corresponding populations are: 6/7 – 9 (50%), 4 – 7 (46%), 2 – 7 (4%) for CSSA/EM and 6 – 9 (65%) for TSSA/EM. Interestingly, a totally unrestrained CSSA/EM calculation predicts the following helix distribution: 2/3 – 9/10 (20%), 5 – 8/9 (14%), 2/3 – 6/7 (10%), 4 – 6 (10%), 4 – 8/9 (4%), 6/7 – 9 (4%), 5 – 12 (2%), 10 – 12 (2%).

In order to check whether the fluctuation in the helical pattern observed in experimentally restrained models derives from intrinsic conformational behaviour of the peptide rather than from inconsistency in or lack of NMR data, 1-ns unrestrained MD simulations of the best conformers obtained from CSSA/EM calculations in both solvents were run in water. These simulations show that the sampled conformations are substantially stable on the simulated timescale, but that they exhibit local fluctuations in the helical pattern on a 10 – 11-ps timescale. These fluctuations are fully comparable to those observed within the TSSA and CSSA structure sets.

Hydrogen bond analysis (see the Supporting Information) shows that, in spite of the different relative magnitudes of atomic interactions expected in vacuo (CSSA, TSSA) and with explicit solvent (MD in water), a substantially convergent picture of the interaction pattern is obtained. Indeed, in CD_3CN/H_2O the identified $O_i - H_{i+4}$ α-helical pattern involves residues from Asp1 to Met8, with a possible C-terminal locking through the formation of $O_i - H_{i+3}$ hydrogen bonds up to the Cys7 – Gly10 pair. A fairly frequent $O_i - H_{i+3}$ hydrogen bond also occurs between the Gly10 and Tyr13 residues. The observed pattern in pure water shows a shifted, shorter, but more stable α-helical pattern, which ranges from Met4 to Gly10. In addition, a long-range hydrogen-bond interaction is detected in one or more

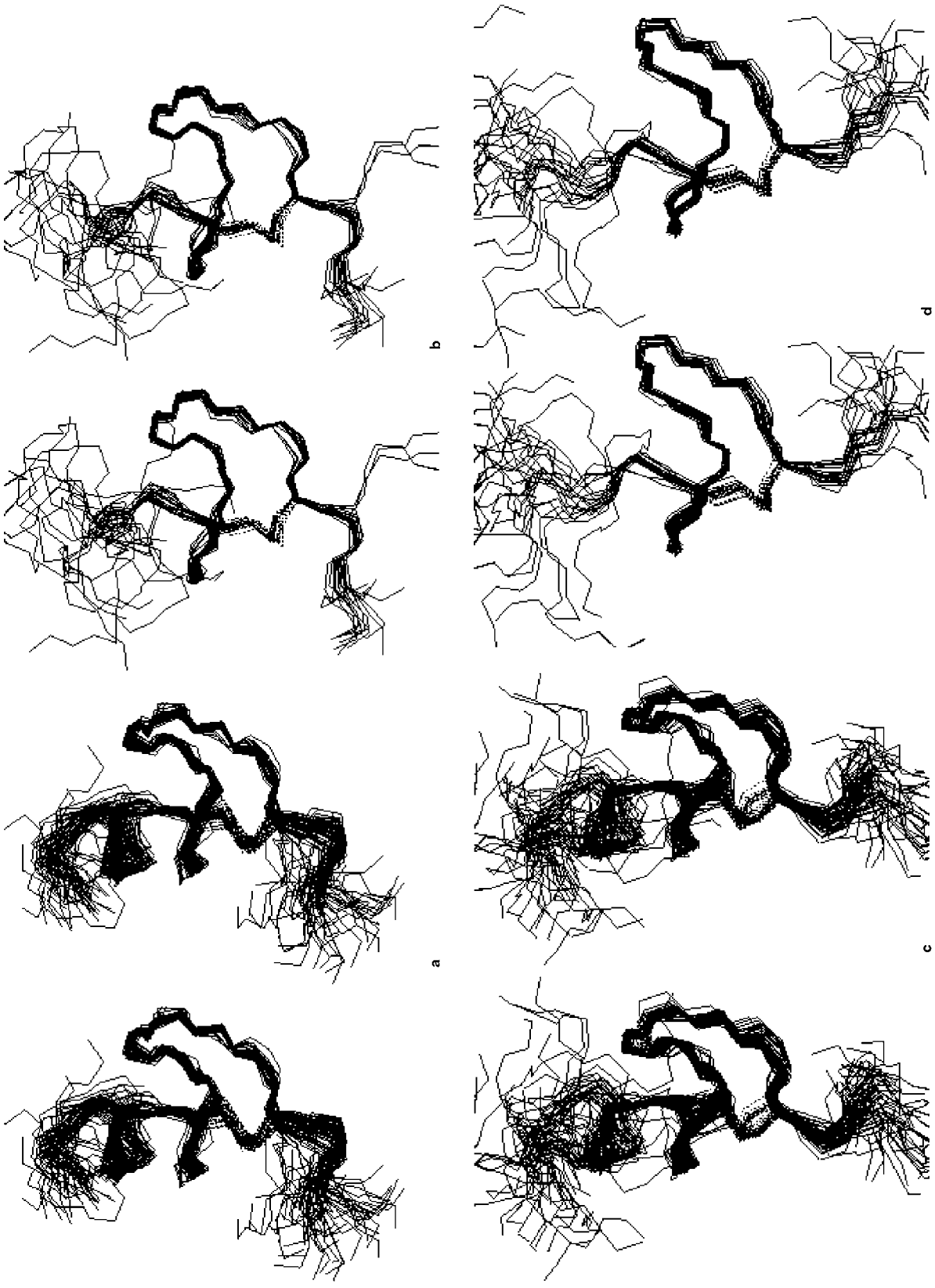

Figure 3. *Stereo drawings of the backbone superposition (residues 7 – 16 of the hMCH peptide) of: a) 50 structures obtained after CSSA/EM from CD_3CN/H_2O data, b) 20 structures obtained after TSSA/EM from CD_3CN/H_2O data, c) 50 structures obtained after CSSA/EM from H_2O data, and d) 20 structures obtained after TSSA/EM from H_2O data. The Cys side chains are represented by dashed lines.*

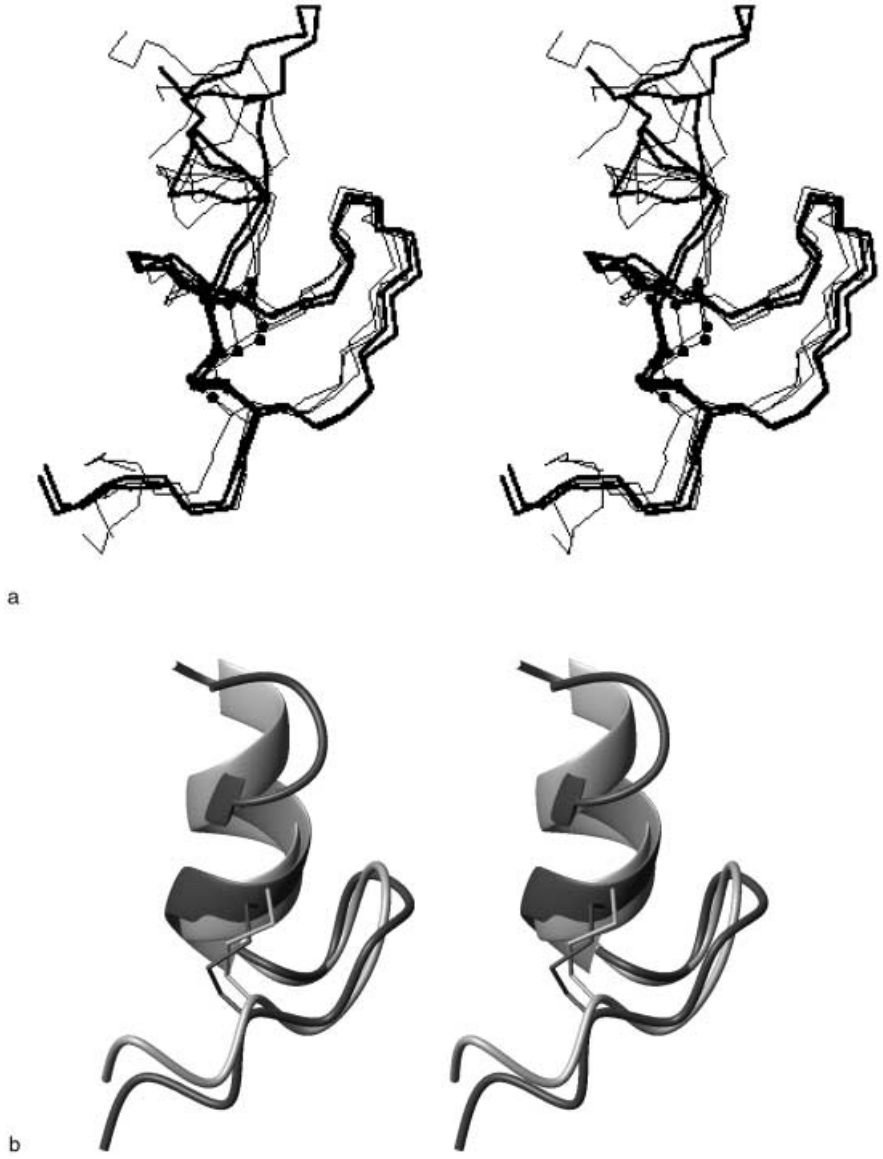

Figure 4. *a) Stereo drawing of the backbone superposition (residues 7 – 16 of the hMCH peptide) of the representative structures obtained from CD_3CN/H_2O data after CSSA/EM and TSSA/EM; the side-chain atoms of Cys residues are represented as filled circles. b) Cartoon models of the representative structures of the main clusters for the 7 – 16 region of the MCH peptide obtained from CD_3CN/H_2O data after CSSA/EM and TSSA/EM.*

structural sets: Cys7 – Cys16 (CSSA/EM in both solvents, MD in H_2O), Gly10 – Cys16 (TSSA/EM in H_2O), or Arg6 – Tyr13 (CSSA/EM in CD_3CN/H_2O).

Comparative analysis of ϕ,ψ torsion angles in the two solvents shows that: 1) Gly10 is found in the γ turn conformation in CD_3CN/H_2O and in the γ turn/3_{10L} helix in pure water, 2) Val12 is in an α_R helix in CD_3CN/H_2O and in an α_R helix/extended conformation in water, 3) Arg14 is found in the extended conformation, 4) Cys16 is α_R-helical in CD_3CN/H_2O and α_R-helical/semi-extended in pure water, and 5) Trp17 is 3_{10L}-helical in CD_3CN/H_2O and semi-extended in water.

The conformational analysis of the representative structures of the main clusters for hMCH shows some common features for the residues required for the formation of the MCH peptide/receptor complex (Arg6, Met8, Arg11, and Tyr13; Figure 5). In particular, it may be noted that:

a) Met8 is found in the α_R-helical conformation in all cases
b) Arg11 is α-helical in CD_3CN/H_2O solution and α-helical/semi-extended in water solution
c) Arg6 is semi-extended or α_R-helical
d) the Tyr13 residue is in the semi-extended or the 3_{10L} helix conformation
e) the Arg6, Tyr13, and Arg11 side chains are in close spatial proximity. In particular, the aromatic ring of Tyr13 lies between the two side chains of Arg6 and Arg11, very close to Arg6. The two Arg residues, together with the Arg14 side chain, form a positively charged triangle, with Tyr13 protruding out of this otherwise hydrophilic face of the molecule, where the Asp3 is also located
f) the Met8 side chain points in the opposite direction with respect to the plane in (e), and is located in the middle of a hydrophobic surface almost parallel to the hydrophilic one.

It is important to note that the side chains of the residues critical for the biological activity overlap well along the cluster in CD_3CN/H_2O and in water solution. These structural elements are potentially important for defining the three-dimensional surface for the peptide interaction with its receptor.

Discussion

The three-dimensional structural determination of MCH is mainly aimed towards obtaining reliable structure – activity relationships for subsequent modeling of complexes with the receptor and/or for the design of new bioactive analogues. We characterized the hMCH solution structure by NMR spectroscopy in two different environments (pure water and a CD_3CN/H_2O (1:1 v/v) mixture), which usually gives rise to substantial conformational differences in small and medium-sized peptides. We minimized any conformational biasing deriving from the computational method by using several computational approaches with widely varied relative weights of theoretical versus experimental information, and we specifically aimed the final analyses of the resulting structures towards checking of model robustness and identification of common and unequivocal conformational features of this peptide in different solvent environments. In addition, the CD data analysis in CD_3CN/H_2O gives a helical content (19%) that is in good agreement with the

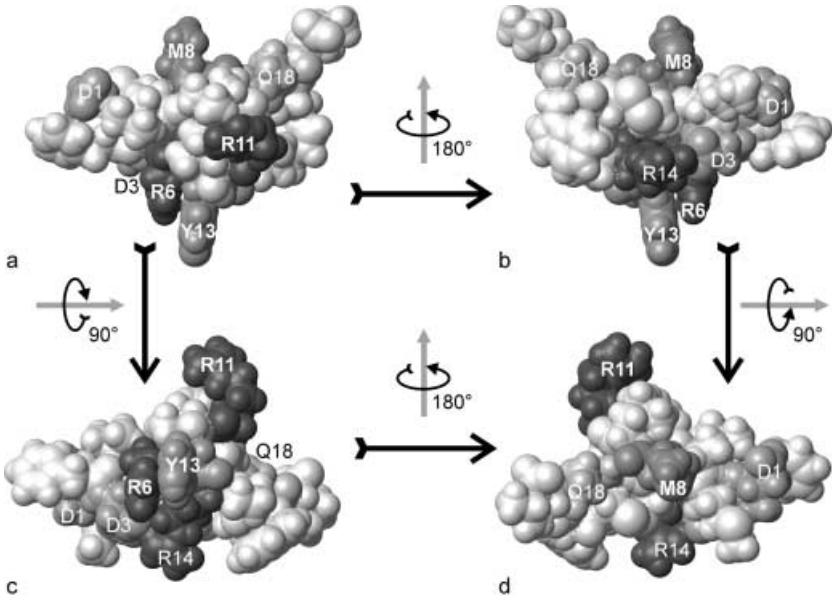

Figure 5. *Side-chain orientations of selected MCH residues. The van der Waals surface of the representative conformer of the most populated cluster in CD_3CN/H_2O is shown. Both biologically relevant (bold labels) and polar residues are labeled (with one-letter amino acid code and residue number) and shaded as follows: Arg residues are shown in dark grey, Met8 and Tyr13 in medium-dark grey, Asp in medium grey, Gln18 in light grey, and the other (hydrophobic) residues in very light grey.*

findings obtained from NMR spectroscopy and computational results.

Our results indicate the existence of a stable fold of hMCH, relatively insensitive to experimental conditions. Therefore, these findings represent an important step towards an understanding of the structure – activity relationship for this class of bioactive molecules.

A careful comparison of the structures obtained in the two solvents shows that these structures are substantially different from that reported by Brown and co-workers[25, 26] for the cyclic MCH(5 – 14) subunit of salmon MCH, and later used to perform a molecular characterization of the MCH/receptor complex.[27] In particular, the NMR and MD data for our structures do not confirm the structural element that stabilizes the protein: the Tyr phenolic OH group is not close to the Cys and Met carbonyl oxygen atoms and is not involved in any hydrogen bonds with these atoms. This finding is in agreement with the good activity of the [Phe13]MCH analogue and the involvement of the residue at position 13 in hydrophobic interactions with the receptor.[22]

The major difference between the structures in the two environments is the extension of the N-terminal helix. This evidence confirms that the structure of residues 1 – 5 is not important for the binding activity, as reported in the literature.[23, 24] In contrast, the substantial conformational similarities of the hMCH cyclic segments in CD_3CN/H_2O and H_2O suggest a possible biological importance of the three-dimensional structure obtained.

In conclusion, these conformational data require a critical revision of the proposed MCH/receptor complex model.[27] Modeling of both MCH receptors and their complexes with hMCH is currently in progress.

Experimental Section

Peptide synthesis: The hMCH peptide was synthesized by solid-phase methods, by use of standard Fmoc chemistry on a model PSSM8 (Shimadzu) peptide synthesizer. The peptide was obtained by starting from 2-chlorotrityl resin (0.83 mmol g^{-1}).[34]

The α-amino acids were activated in situ by the standard benzotriazol-1-yloxy-tris-pyrrolidino-phosphonium/1-hydroxybenzotriazole/*N*,*N*-diisopropylethylamine (DIEA) procedure;[35] in the cases of the difficult couplings of Asp1, Phe2, Asp3, Met4, Arg6, Cys7, Arg14, Pro15, Cys16, Trp17, and Gln18 the more effective 2-(1*H*-9-azabenzotriazol-1-yl)-1,1,3,3-tetramethyluronium/DIEA mixture was used.[36] Each residue was subjected to the coupling conditions twice for 1 h followed by 5-min treatment with acetic anhydride and pyridine in *N*,*N*-dimethylformamide to cap unreacted amine groups.

The final peptide deprotection and cleavage from the resin was achieved by use of a TFA/H_2O/phenol/thioanisole/ethanedithiol/triisopropylsilane mixture (80:5:5:5:2.5:2.5 v/v, 3 h). The resin was filtered and the filtrate was concentrated. The peptide was then precipitated with cold diethyl ether, dissolved in the water/acetonitrile mixture and lyophilized.

The linear crude peptide was analyzed by RP-HPLC performed on a Shimadzu LC instrument equipped with a SPDM AV-10 diode array and a SIL-10A autosampler. A Phenomenex C_{18} column (4.6 × 250 mm, 5 μm, 300 Å) was used, eluted with a H_2O/0.1% TFA (A) and CH_3CN/0.1% TFA (B) linear gradient (from 20 to 70% B over 30 min, at 1 mL min^{-1} flow rate). The analysis showed a main peak with $R_t = 17.3$. The peptide identity was confirmed by mass MALDI-TOF spectrometric analysis, which gave the expected molecular ion peak $[M-H]^+$ of 2388.

The linear peptide was dissolved in H_2O/CH_3CN (70:30) before purification because of solubility problems and was cyclized by air oxidation under strong agitation for 48 h at room temperature and pH 8.0.

The reaction mixture, analyzed by RP-HPLC, showed a main peak with $R_t = 16.3$. It was then purified on a Waters Delta Prep 4000 instrument equipped with a Waters model 441 UV detector (Vydac C_{18} column, 220 × 150 mm, 15 μm, 300 Å) with the linear gradient described above.

The collected fractions containing the peptide were lyophilized and analyzed by use of the MALDI-TOF Perseptive spectrometer, which gave a molecular ion peak $[M-H]^+$ of 2386.

CD experiments: The CD spectra were obtained at room temperature on a Jasco model J-710 spectropolarimeter. The spectra were collected over the 192 – 260-nm range in a 1-cm path-length cuvette.

The peptide solution was prepared by starting from a stock solution (1.32×10^{-3} M), the concentration of which was calculated spectrophotometrically from the reported extinction coefficients at 280 nm for Tyr (1490 $mol^{-1} dm^3 cm^{-1}$) and Trp (5500 $mol^{-1} dm^3 cm^{-1}$).[37] The stock solution was then diluted with CH_3CN/H_2O (1:1 v/v) to give the final concentration of 6.91×10^{-6} M.

NMR experiments: Two solutions of peptide MCH of about 1.3×10^{-3} M concentration were prepared for the NMR studies by

dissolving the samples either in the H_2O (10% D_2O)/CD_3CN mixture (500 μL, 50:50 v/v) or in neat H_2O (10% D_2O; 500 μL). All deuterated solvents were purchased from Isotec Inc. (Milwaukee, WI, USA). CD_3CN had a 99.96% relative isotopic abundance of deuterium. NMR experiments were carried out on a Varian Inova 600 MHz spectrometer, operating at a ^1H resonance frequency of 600 MHz, equipped with a triple axis PFG probe optimized for ^1H detection (located at the Istituto di Biostrutture e Bioimmagini, CNR, Napoli (Italy)). All 2D spectra were recorded by the States–Haberkorn method; water suppression was obtained by presaturation of the solvent line during the recycle delay (2.5 s) or by the WATERGATE PFG technique.

2D-TOCSY experiments were recorded at 298, 302, and 307 K by the use of a MLEV17 mixing scheme of 70 ms (spectral width 7000 Hz both along f_1 and f_2, 4096 × 256 data points in t_2 and t_1, respectively, 16 scans per t_1 increment). The 2D-NOESY spectra used to derive the geometric constraints were measured at 298 K by the standard pulse sequence with mixing times of 200 and 250 ms (spectral width 7000 Hz both along f_1 and f_2, 4096 × 256 data points in t_2 and t_1 respectively, 64 scans per t_1 increment). The 2D-ROESY spectrum was recorded at 298 K with a mixing time of 100 ms and the continuous wave method for mixing (spectral width 7000 Hz both along f_1 and f_2, 4096 × 256 data points in t_2 and t_1, respectively, 64 scans per t_1 increment). The 2D DQF-COSY experiment was obtained with saturation of the water signal during the relaxation period (spectral width 7000 Hz both along f_1 and f_2, 4096 × 256 data points in t_2 and t_1, respectively, 256 scans per t_1 increment).

The data were typically apodized with a square cosine window function and zero-filled to 1 K in f_1 prior to Fourier transformation. Chemical shifts were referenced to CD_3CN to 2.0 ppm and, in the case of H_2O/D_2O solution, to external tetramethylsilane ($\delta = 0$ ppm). The complete assignments of the peptide have been deposited at the BioMagResBank under accession number 5523.

Measurements of coupling constants were obtained from 1D data, collected with a spectral width of 7000 Hz, 16 K data points zero-filled to 32 K prior to Fourier transformation, and from DQF-COSY, after zero-filling to 8 K in ω_2.

The possible occurrence of aggregation was tested by measuring chemical shifts in the 1D spectrum and analyzing the cross-peak patterns in two NOESY spectra recorded with a peptide concentration of 0.5 mM.

Data were transformed with the standard Varian software and then processed with the XEASY program.[38]

Computational details: Experimental distance restraints for structure calculations were derived from cross-peak intensities in NOESY spectra (200 ms) recorded in H_2O and H_2O/CD_3CN. NOESY cross-peaks were manually integrated by use of the XEASY program and converted to upper distance constraints according to an inverse sixth power peak volume-to-distance relationship for the backbone and an inverse fourth power function for side chains by use of the CALIBA module of the DYANA program. Additional upper and lower distance limits were inserted between the two Cys thiol groups. Distance constraints were then used by the GRIDSEARCH module, also implemented in DYANA, to generate a set of allowable dihedral angles. Constraints that involved fixed distances and inviolable constraints were removed, and the structure calculation was carried out with the macro ANNEAL, by use of torsion angle dynamics. 100 structures were calculated by TSSA, starting with a total of 4000 MD steps and a default value of maximum temperature (8 target function units per degree of freedom). The 20 best structures in terms of target function were refined by 2000 restrained EM steps with a combination of steepest descent and conjugate gradient algorithms, by use of the SANDER–CLASSIC module of AMBER 6.0[39] with the AMBER all-atom 1991 parameterization, a distance-dependent dielectric constant $\varepsilon = r_{ij}$, and a cut-off radius of 8 Å for nonbonded interactions. A reduced net charge on charged residues (20% of its original value) was used to mimic the solvent shielding effect. Distance restraints are represented by a well with a square bottom with 0.5-Å-thick parabolic sides (force constant of 20 kcal mol^{-1} Å^{-1}), which is then smoothly converted into linear form.

The selected structures were also subjected to unrestrained EM, by using the same protocol and parameters, in order to identify potential trapping of the models in high-energy conformations and to detect any large inconsistencies due to conformational equilibria and/or wrong assignments. For the same purpose, and to characterize the intrinsic conformational preferences of the peptide in the selected simulation conditions, a set of totally unrestrained CSSA/EM calculations was also run. In each set, the sampled structures were clustered by best-fitting of the backbone atoms of residues from Cys7 to Cys16 with the program MOLMOL.[40] Representative structures of the most populated clusters were used as starting structures for restrained CSSA. SA cycles of five runs of 500000 molecular dynamics (MD) steps each were run with a time step of 0.0015 ps and $T_{max} = 800$ K. Data were collected for analysis every 50000 steps. The SHAKE procedure,[41] which performs bond-length constraints, was used for all calculations. Each CSSA cycle produced 50 structures, which were used after EM for clustering and analysis.

To identify further potential inconsistencies and high-energy minima problems, and to characterize the intrinsic conformational preferences of the peptide under the selected simulation conditions, a set of totally unrestrained CSSA/EM calculations was also run.

The representative structures of the main clusters identified in CSSA/EM runs were solvated in isometric truncated octahedron boxes of TIP3 water molecules[42] (box size 47.8 Å, which corresponds to 2605 water molecules for the structure in H_2O, and a box size of 48.3 Å, which corresponds to 2699 water molecules for the structure in CD_3CN/H_2O) with a clearance of 10 Å in each direction after addition of a Cl^- ion to ensure electrostatic neutrality. An initial round of constrained EM (2000 steps) and MD (100 ps) equilibration was used to relax the solvent, followed by 250 ps of restrained MD with a force constant of 8 kcal mol^{-1} Å^{-1}, 250 ps of unrestrained MD equilibration and, finally, 1 ns of unrestrained MD production run, collecting coordinates, velocities, and energies every 500 steps for analysis. Both the last 200 ps of restrained MD and 1 ns of unrestrained MD were subjected to subsequent analysis.

MD in a solvent box was performed with the SANDER module of the AMBER 6.0 package, with the AMBER all-atom 1994 parameterization,[43] a dielectric constant $\varepsilon = 1$, and a cut-off radius of 8 Å for nonbonded interactions. The Particle Mesh Ewald approach was used to allow for long-range electrostatic interactions,[44] with a charge-grid density of 0.95 Å, cubic spline interpolation, and a direct sum tolerance of 10^{-5}. Covalent bonds involving hydrogen atoms were constrained to constant values by use of the SHAKE algorithm, which allowed the use of a 2-fs integration time step. Simulations were performed in the NTP ensemble ($T = 300$ K and $p = 1$ atm).

The analysis modules of both the AMBER 6.0 package and the MOLMOL program were used for structural analysis, while the validation of the final structures was obtained with the aid of the PROCHECK 3.5.4 program.[45]

This work was supported by the National Research Council "Progetto Biotecnologie: Biotecnologie Industriali e Metodiche Innovative, Legge 95/95". Dr. Giuseppe Perretta, Mr. Leopoldo Zona, and Mr. Luca De Luca are acknowledged for technical assistance.

[1] H. Kawauchi, I. Kawazoe, M. Tsubokawa, M. Kishida, B. I. Baker, *Nature* **1983**, *305*, 321 – 323.
[2] B. I. Baker, *Int. Rev. Cytol.* **1991**, *12*, 1 – 47.
[3] F. Presse, I. Sorokovsky, J. P. Max, S. Nicolandis, J. L. Nahor, *Neuroscience* **1996**, *71*, 735 – 745.
[4] D. Qu, D. S. Ludwig, S. Gammeltoft, M. Piper, M. A. Pelleymounter, M. J. Cullen, W. F. Mathes, J. Przupek, R. Kanarek, E. Maratos-Flier, *Nature* **1996**, *380*, 243 – 247.
[5] C. Rovère, A. Viale, J. L. Nahon, P. Kitahan, *Endocrinology* **1996**, *137*, 2954 – 2958.
[6] M. Rossi, S. J. Choi, D. O'Shea, T. Miyoshi, M. A. Ghatei, S. R. Bloom, *Endocrinology* **1997**, *138*, 351 – 355.
[7] M. I. Gonzalez, S. Vaziri, C. A. Wilson, *Peptides* **1996**, *17*, 171 – 177.
[8] M. I. Gonzalez, V. Kalia, D. R. Hole, C. A. Wilson, *Peptides* **1997**, *18*, 387 – 392.
[9] M. Shimada, N. A. Tritos, B. B. Lowell, J. S. Flier, E. Maratos-Flier, *Nature* **1998**, *396*, 670 – 674.
[10] D. S. Ludwig, K. G. Mountjoy, J. B. Tatro, J. A. Gillette, R. C. Freferich, J. S. Flier, E. Maratos-Flier, *Am. J. Physiol.* **1998**, *274*, E627 – E633.
[11] J. Chambers, R. S. Ames, D. Bergsma, A. Muir, L. R. Fitzgerald, G. Hervieu, G. M. Dytko, J. J. Foley, J. Martin, W-S. Liu, J. Park, C. Ellis, S. Ganguly, S. Konchar, J. Chunderay, R. Leslie, S. Wilson, H. M. Sarau, *Nature* **1999**, *400*, 261 – 265.
[12] D. Bachner, H. Kreienkamp, C. Weise, F. Buck, D. Richter, *FEBS Lett.* **1999**, *457*, 522 – 524.
[13] P. M. Lembo, E. Grazzini, J. Cao, D. A., Hubatsch, M. Pelletier, C. Hoffert, S. St-Onge, C. Pou, J. Labrecque, T. Grobleswky, D. O'Donnell, K. Payza, S. Ahmad, P. Walker, *Nat. Cell. Biol.* **1999**, *1*, 267 – 271.
[14] Y. Saito, H-P. Nothacker, Z. Wang, S. H. S. Lin, P. Leslie, O. Civelli, *Nature* **1999**, *400*, 265 – 269.
[15] Y. Saito, H. P. Nothacker, O. Civelli, *TEM* **2000**, *11*, 299 – 303.
[16] M. Mori, M. Harada, Y. Terao, T. Sugo, T. Wanabe, Y. Shimomura, M. Abe, Y. Shintani, H. Onda, O. Nishimura, M. Fujino, *Biochem. Biophys. Res. Commun.* **2001**, *283*, 1013 – 1018.
[17] J. Hill, M. Duckworth, P. Murdock, G. Rennie, C. Sabido-David, R. S. Ames, P. Szekeres, S. Wilson, D. J. Bergsma, I. S. Gloger, D. S. Levy, J. K. Chambers, A. I. Muir, *J. Biol. Chem.* **2001**, *276*, 20 125 – 20 129.
[18] A. W. Sailer, H. Sano, Z. Zeng, T. P. McDonald, J. Pan , S. S. Pong, S. D. Feighner, C. P. Tan, T. Fukami, H. Iwaasa, D. L. Hreniuk, N. R. Morin, S. J. Sadowsky, R. Nossoughi, M. Ito, M. Ito, A. Bansal, B. Ky, D. J. Figueroa, Q. Jiang, C. P. Austin, D. J. MacNeil, A. Ishihara, M. Ihara, A. Kanatani, L. H. T. Van der Ploeg, A. D. Howard, Q. Liu, *Proc. Natl. Acad. Sci. USA* **2001**, *98*, 7564 – 7569.
[19] C. D. Strader, I. S. Sigal, R. B. Register, M. R. Candelore, E. Rands, R. A. F. Dixon, *Proc. Natl. Acad. Sci. USA* **1987**, *84*, 4384 – 4388.
[20] M. E. Hadley, C. Zechel, B. C. Wilkes, A. M. Castrucci, M. A. Visconti, M. Pozo-Alonso, V. J. Hruby, *Life Sci.* **1987**, *40*, 1139 – 1145.
[21] R. Drozdz, E. Hintermann, H. Tanner, U. Zumsteg, A. N. Eberle *J. Pept. Sci.* **1999**, *5*, 234 – 242.
[22] V. Audinot, P. Beauverger, C. Lahaye, T. Suply, M. Rodriguez, C. Ouvry, V. Lamamy, J. Imbert, H. Rique, J. L. Nahon, J. P. Galizzi, E. Canet, N. Levens, J. L. Fauchere, J. A. Boutin, *J. Biol. Chem.* **2001**, *276*, 13 554 – 13 562.
[23] M. A. Bednarek, S. D. Feighner, D. L. Hreniuk, O. C. Palyha, N. R. Morin, S. J. Sadowski, D. J. MacNeil, A. D. Howard, L. H. Y. van der Ploeg, *Biochemistry* **2001**, *40*, 9379 – 9386.
[24] M. A. Bednarek, C. Tan, D. L. Hreniuk, O. C. Palyha, L. H. Y. Van der Ploeg, *J. Biol. Chem.* **2002**, *277*, 13 821 – 13 826.
[25] D. W. Brown, N. M. Campbell, R. G. Kinsman, P. D. White, C. A. Moss, D. J. Osguthorpe, P. K. C. Paul, B. I. Baker, *Biopolymers* **1990**, *29*, 609 – 622.
[26] P. K. C. Paul, P. Dauber-Osguthorpe, M. M. Campbell, D. W. Brown, R. G. Kinsman, C. Moss, D. J. Osguthorpe, *Biopolymers* **1990**, *29*, 623 – 637.
[27] D. MacDonald, N. Murgolo, R. Zhang, J. P. Durkin, X. Yao, C. D. Strader, M. P. Graziano, *Mol. Pharmacol.* **2000**, *58*, 217 – 225.
[28] N. Sreerama, R. W. Woody, *Anal. Biochem.* **2000**, *287*, 252 – 260.
[29] C. Griesinger, G. Otting, K. Wüthrich, R. R. Ernst, *J. Am. Chem. Soc.*, **1988**, *110*, 7870 – 7872.
[30] M. Rance, O. W. Sørensen, G. Bodenhausen, G. Wagner , R. R. Ernst, K. Wüthrich, *Biochem. Biophys. Res. Commun.* **1983**, *117*, 479 – 485.
[31] A. Kumar, R. R. Ernst, K. Wüthrich, *Biochem. Biophys. Res. Commun.* **1980**, *95*, 1 – 6.
[32] K. Wüthrich, *NMR of Proteins and Nucleic Acids*, **1986**, Wiley, New York.
[33] P. Güntert, C. Mumenthaler, K. Wüthrich, *J. Mol. Biol.*, **1997**, *273*, 283 – 298.
[34] K. Barlos, O. Chatzi, D. Gatos, G. Stavropoulos, *Int. J. Peptide Protein Res.* **1991**, *37*, 513 – 520.
[35] J. Coste, D. Le-Nguyen, B. Castro, *Tetrahedron Lett.* **1990**, *31*, 201 – 208.
[36] L. A.Carpino, *J. Am. Chem. Soc.* **1993**, *115*, 4397 – 4398.
[37] C. N. Pace, F. Vajdos, L. Fee, G. Grimsley, T. Gray, *Protein Sci.* **1995**, *4*, 2411 – 2423.
[38] C. Bartels, T. Xia, M. Billeter, K. Wüthrich, *J. Biomol. NMR* **1995**, *5*, 1 – 10.
[39] D. A. Case, D. A. Pearlman, J. W. Caldwell, T. E. Cheatham III, W. S. Ross, C. L. Simmerling, T. A. Darden, K. M. Merz, R. V. Stanton, A. L. Cheng, J. J. Vincent, M. Crowley, V. Tsui, R. J. Radmer, Y. Duan, J. Pitera, I. Massova, G. L. Seibel, U. C. Singh, P. K. Weiner, P. A. Kollman, *AMBER 6* **1999**, University of California, San Francisco.
[40] R. Koradi, M. Billeter, K. Wüthrich, *J. Mol. Graphics* **1996**, *14*, 51 – 55.
[41] J. P. Ryckaert, G. Ciccotti, H. J. C. Berendsen, *J. Comput. Phys.* **1977**, *23*, 327 – 341.
[42] W. L. Jorgensen, J. Chandrasekhar, J. Madura, M. L. Klein, *J. Chem. Phys.* **1983**, *79*, 926 – 935.
[43] W. D. Cornell, P. Cieplak, C. I. Bayly, I. R. Gould, K. M. Merz Jr., D. M. Ferguson, D. C. Spellmeyer, T. Fox, J. W. Caldwell, P. A. Kollman, *J. Am. Chem. Soc.* **1995**, *117*, 5179 – 5197.
[44] D. M. York, T. A. Darden, L. G. Pedersen, *J. Chem. Phys.* **1993**, *99*, 8345 – 8348.
[45] R. A. Laskowski, M. W. MacArthur, D. S. Moss, J. M. Thornton, *J. Appl. Cryst.* **1993**, *26*, 283 – 291.

Received: May 31, 2002
Revised version: September 17, 2002 [F 427]